

$B^0 \rightarrow \pi^+\pi^-\pi^0$ Time Dependent Dalitz analysis at BaBar.

Gianluca Cavoto*

INFN Sezione di Roma, Piazzale Aldo Moro 2, 00185 Rome, Italy

I present here results of a time-dependent analysis of the Dalitz structure of neutral B meson decays to $\pi^+\pi^-\pi^0$ from a dataset of 346 million $B\bar{B}$ pairs collected at the $\Upsilon(4S)$ center of mass energy by the BaBar detector at the SLAC PEP-II e^+e^- accelerator. No significant CP violation effects are observed and 68% confidence interval is derived on the weak angle α to be [75,152]

I. INTRODUCTION

The time-dependent analysis of the $B^0 \rightarrow \pi^+\pi^-\pi^0$ Dalitz plot (DP), dominated by the $\rho(770)$ intermediate resonances, extracts simultaneously the strong transition amplitudes and the weak interaction phase $\alpha \equiv \arg[-V_{td}V_{tb}^*/V_{ud}V_{ub}^*]$ of the Unitarity Triangle [1]. In the Standard Model, a non-zero value for α is responsible for the occurrence of mixing-induced CP violation in this decay. $\rho^\pm\pi^\mp$ is not a CP eigenstate, and four flavor-charge configurations ($B^0(\bar{B}^0) \rightarrow \rho^\pm\pi^\mp$) must be considered. The corresponding isospin analysis [2] is unfruitful with the present statistics since two pentagonal amplitude relations with 12 unknowns have to be solved (compared to 6 unknowns for the $\pi^+\pi^-$ and $\rho^+\rho^-$ systems).

The differential B^0 decay width with respect to the Mandelstam variables s_+ , s_- (*i.e.*, the Dalitz plot [3]) reads $d\Gamma(B^0 \rightarrow \pi^+\pi^-\pi^0) = \frac{1}{(2\pi)^3} \frac{|A_{3\pi}|^2}{8m_{B^0}^2} ds_+ ds_-$, where $A_{3\pi}$ ($\bar{A}_{3\pi}$) is the Lorentz-invariant amplitude of the three-body decay $B^0 \rightarrow \pi^+\pi^-\pi^0$ ($\bar{B}^0 \rightarrow \pi^+\pi^-\pi^0$). We assume in the following that the amplitudes are dominated by the three resonances ρ^+ , ρ^- and ρ^0 and we write $A_{3\pi} = f_+A^+ + f_-A^- + f_0A^0$ and $\bar{A}_{3\pi} = f_+\bar{A}^+ + f_-\bar{A}^- + f_0\bar{A}^0$, where the f_κ (with $\kappa = \{+, -, 0\}$ denoting the charge of the ρ from the decay of the B^0 meson) are functions of s_+ and s_- that incorporate the kinematic and dynamical properties of the B^0 decay into a (vector) ρ resonance and a (pseudoscalar) pion, and where the A^κ are complex amplitudes that include weak and strong transition phases and that are independent of the Dalitz variables.

With $\Delta t \equiv t_{3\pi} - t_{\text{tag}}$ defined as the proper time interval between the decay of the fully reconstructed $B_{3\pi}^0$ and that of the other meson B_{tag}^0 , the time-dependent decay rate

when the tagging meson is a B^0 (\bar{B}^0) is given by

$$|\mathcal{A}_{3\pi}^\pm(\Delta t)|^2 = \frac{e^{-|\Delta t|/\tau_{B^0}}}{4\tau_{B^0}} \left[|A_{3\pi}|^2 + |\bar{A}_{3\pi}|^2 \mp (|A_{3\pi}|^2 - |\bar{A}_{3\pi}|^2) \cos(\Delta m_d \Delta t) \pm 2\text{Im}[\bar{A}_{3\pi}A_{3\pi}^*] \sin(\Delta m_d \Delta t) \right], \quad (1)$$

where τ_{B^0} is the mean B^0 lifetime and Δm_d is the $B^0\bar{B}^0$ oscillation frequency. Here, we have assumed that CP violation in \bar{b} mixing is absent ($|q/p| = 1$), $\Delta\Gamma_{B_d} = 0$ and CPT is conserved. Inserting the amplitudes $A_{3\pi}$ and $\bar{A}_{3\pi}$ one obtains for the terms in Eq. (1)

$$\begin{aligned} |A_{3\pi}|^2 \pm |\bar{A}_{3\pi}|^2 &= \sum_{\kappa \in \{+, -, 0\}} |f_\kappa|^2 U_\kappa^\pm + \\ 2 \sum_{\kappa < \sigma \in \{+, -, 0\}} & (\text{Re}[f_\kappa f_\sigma^*] U_{\kappa\sigma}^{\pm, \text{Re}} - \text{Im}[f_\kappa f_\sigma^*] U_{\kappa\sigma}^{\pm, \text{Im}}), \\ \text{Im}(\bar{A}_{3\pi}A_{3\pi}^*) &= \sum_{\kappa \in \{+, -, 0\}} |f_\kappa|^2 I_\kappa + \\ \sum_{\kappa < \sigma \in \{+, -, 0\}} & (\text{Re}[f_\kappa f_\sigma^*] I_{\kappa\sigma}^{\text{Im}} + \text{Im}[f_\kappa f_\sigma^*] I_{\kappa\sigma}^{\text{Re}}), \quad (2) \end{aligned}$$

The 27 real-valued coefficients defined in Tab.IV that multiply the $f_\kappa f_\sigma^*$ bilinears are determined by the fit. Each of the coefficients is related in a unique way to physically more intuitive quantities, such as tree-level and penguin-type amplitudes, the angle α , or the quasi-two-body CP and dilution parameters [4] (*cf.* Section IV B). We determine the quantities of interest in a subsequent least-squares fit to the measured U and I coefficients.

II. DALITZ MODEL

The ρ resonances are assumed to be the sum of the ground state $\rho(770)$ and the radial excitations $\rho(1450)$ and $\rho(1700)$, with resonance parameters determined by a combined fit to $\tau^+ \rightarrow \bar{\nu}_\tau \pi^+ \pi^0$ and $e^+e^- \rightarrow \pi^+\pi^-$ data [5]. Since the hadronic environment is different in B decays, we cannot rely on this result and therefore determine the relative $\rho(1450)$ and $\rho(1700)$ amplitudes simultaneously with the CP parameters from the fit. Variations of the other parameters and possible contributions

*Electronic address: gianluca.cavoto@roma1.infn.it

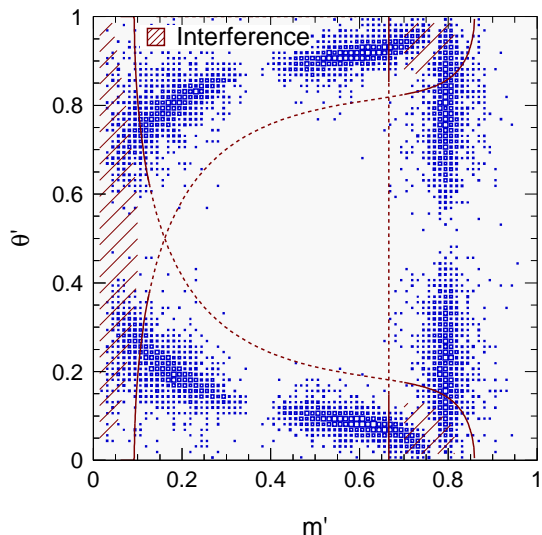


FIG. 1: Square Dalitz plots for Monte-Carlo generated $B^0 \rightarrow \pi^+ \pi^- \pi^0$ decays. The decays have been simulated without any detector effect and the amplitudes A^+ , A^- and A^0 have all been chosen equal to 1 in order to have destructive interferences at equal ρ masses. The main overlap regions between the charged and neutral ρ bands are indicated by the hatched areas. Dashed lines in both plots correspond to $\sqrt{s_{+,-,0}} = 1.5 \text{ GeV}/c^2$: the central region of the Dalitz plot contains almost no signal event.

to the $B^0 \rightarrow \pi^+ \pi^- \pi^0$ decay other than the ρ 's are studied as part of the systematic uncertainties (Section IV A).

Following Ref. [5], the ρ resonances are parameterized in f_κ by a modified relativistic Breit-Wigner function introduced by Gounaris and Sakurai (GS) [6].

Large variations occurring in small areas of the Dalitz plot are very difficult to describe in detail. These regions are particularly important since this is where the interference, and hence our ability to determine the strong phases, occurs. We therefore apply the transformation $ds_+ ds_- \rightarrow |\det J| dm' d\theta'$, which defines the *Square Dalitz plot* (SDP). The new coordinates are $m' \equiv \frac{1}{\pi} \arccos\left(2 \frac{m_0 - m_0^{\min}}{m_0^{\max} - m_0^{\min}} - 1\right)$, $\theta' \equiv \frac{1}{\pi} \theta_0$, where m_0 is the invariant mass between the charged tracks, $m_0^{\max} = m_{B^0} - m_{\pi^0}$ and $m_0^{\min} = 2m_{\pi^+}$ are the kinematic limits of m_0 and θ_0 is the ρ^0 helicity angle; θ_0 is defined by the angle between the π^+ in the ρ^0 rest frame and the ρ^0 flight direction in the B^0 rest frame. J is the Jacobian of the transformation that zooms into the kinematic boundaries of the Dalitz plot, shown in Fig. 1.

III. ANALYSIS DESCRIPTION

The U and I coefficients and the $B^0 \rightarrow \pi^+ \pi^- \pi^0$ event yield are determined by a maximum-likelihood fit of the signal model to the selected candidate events. Kinematic and event shape variables exploiting the characteristic properties of the events are used in the fit to discriminate

signal from background.

A. Signal and background parametrization

We reconstruct $B^0 \rightarrow \pi^+ \pi^- \pi^0$ candidates from pairs of oppositely-charged tracks, which are required to form a good quality vertex, and a π^0 candidate. In order to ensure that all events are within the Dalitz plot boundaries, we constrain the three-pion invariant mass to the B mass.

A B -meson candidate is characterized kinematically by the energy-substituted mass $m_{\text{ES}} = [(\frac{1}{2}s + \mathbf{p}_0 \cdot \mathbf{p}_B)^2 / E_0^2 - \mathbf{p}_B^2]^{\frac{1}{2}}$ and energy difference $\Delta E = E_B^* - \frac{1}{2}\sqrt{s}$, where (E_B, \mathbf{p}_B) and (E_0, \mathbf{p}_0) are the four-vectors of the B -candidate and the initial electron-positron system, respectively. The asterisk denotes the $\Upsilon(4S)$ frame, and s is the square of the invariant mass of the electron-positron system. We require $5.272 < m_{\text{ES}} < 5.288 \text{ GeV}/c^2$. The ΔE resolution exhibits a dependence on the π^0 energy and therefore varies across the Dalitz plot. We account for this effect by introducing the transformed quantity $\Delta E' = (2\Delta E - \Delta E_+ - \Delta E_-) / (\Delta E_+ - \Delta E_-)$, with $\Delta E_{\pm}(m_0) = c_{\pm} - (c_{\pm} \mp \bar{c})(m_0/m_0^{\max})^2$, where m_0 is strongly correlated with the energy of π^0 . We use the values $\bar{c} = 0.045 \text{ GeV}$, $c_- = -0.140 \text{ GeV}$, $c_+ = 0.080 \text{ GeV}$, $m_0^{\max} = 5.0 \text{ GeV}$, and require $-1 < \Delta E' < 1$.

Backgrounds arise primarily from random combinations in continuum $q\bar{q}$ events. To enhance discrimination between signal and continuum, we use a neural network (NN) [7] to combine discriminating topological variables.

The time difference Δt is obtained from the measured distance between the z positions (along the beam direction) of the $B_{3\pi}^0$ and B_{tag}^0 decay vertices, and the boost $\beta\gamma = 0.56$ of the e^+e^- system: $\Delta t = \Delta z / \beta\gamma c$. To determine the flavor of the B_{tag}^0 we use the B flavor tagging algorithm of Ref. [8]. This produces six mutually exclusive tagging categories.

Events with multiple B candidates passing the full selection occur in 16% ($\rho^{\pm}\pi^{\mp}$) and 9% ($\rho^0\pi^0$) of the time, according to signal MC. If the multiple candidates have different π^0 candidates, we choose the B candidate with the reconstructed π^0 mass closest to the nominal π^0 mass; in the case that both candidates have the same π^0 , we pick the first one.

The signal efficiency determined from MC simulation is 24% for $B^0 \rightarrow \rho^{\pm}\pi^{\mp}$ and $B^0 \rightarrow \rho^0\pi^0$ events, and 11% for non-resonant $B^0 \rightarrow \pi^+\pi^-\pi^0$ events.

Of the selected signal events, 22% of $B^0 \rightarrow \rho^{\pm}\pi^{\mp}$, 13% of $B^0 \rightarrow \rho^0\pi^0$, and 6% of non-resonant events are misreconstructed. Misreconstructed events occur when a track or neutral cluster from the tagging B is assigned to the reconstructed signal candidate. This occurs most often for low-momentum tracks and photons and hence the misreconstructed events are concentrated in the corners of the Dalitz plot. Since these are also the areas

where the ρ resonances overlap strongly, it is important to model the misreconstructed events correctly.

We use MC simulated events to study the background from other B decays. More than a hundred channels were considered in preliminary studies, of which twenty-nine are included in the final likelihood model. For each mode, the expected number of selected events is computed by multiplying the selection efficiency (estimated using MC simulated decays) by the world average branching fraction (or upper limit), scaled to the dataset luminosity (310 fb^{-1}). The selected on-resonance data sample is assumed to consist of signal, continuum-background and B -background components, separated by the flavor and tagging category of the tag side B decay. The signal likelihood consists of the sum of a correctly reconstructed (“truth-matched”, TM) component and a misreconstructed (“self-cross-feed”, SCF) component.

B. Dalitz and Δt distribution

The Dalitz plot PDFs require as input the Dalitz plot-dependent relative selection efficiency, $\epsilon = \epsilon(m', \theta')$, and SCF fraction, $f_{\text{SCF}} = f_{\text{SCF}}(m', \theta')$. Both quantities are taken from MC simulation.

Away from the Dalitz plot corners the efficiency is uniform, while it decreases when approaching the corners, where one of the three particles in the final state is close to rest so that the acceptance requirements on the particle reconstruction become restrictive. Combinatorial backgrounds and hence SCF fractions are large in the corners of the Dalitz plot due to the presence of soft neutral clusters and tracks.

The width of the dominant $\rho(770)$ resonance is large compared to the mass resolution for TM events (about $8 \text{ MeV}/c^2$ core Gaussian resolution). We therefore neglect resolution effects in the TM model. Misreconstructed events have a poor mass resolution that strongly varies across the Dalitz plot. It is described in the fit by a 2×2 -dimensional resolution function, convoluted with signal Dalitz PDF.

The Δt resolution function for signal and B -background events is a sum of three Gaussian distributions, with parameters determined by a fit to fully reconstructed B^0 decays [8].

The Dalitz plot- and Δt -dependent PDFs factorize for the charged- B -background modes, but not necessarily for the neutral- B background due to $B^0\bar{B}^0$ mixing.

The charged B -background contribution to the likelihood parametrizes tag-“charge” correlation (represented by an effective flavor-tag-versus-Dalitz-coordinate correlation), and therefore possible direct CP violation in these events.

The Dalitz plot PDFs are obtained from MC simulation and are described with the use of non-parametric functions. The Δt resolution parameters are determined by a fit to fully reconstructed B^+ decays.

The neutral- B background is parameterized with

PDFs that depend on the flavor tag of the event and, depending on the final states they can show correlations between the flavor tag and the Dalitz coordinate. The Dalitz plot PDFs are obtained from MC simulation and are described with the use of non-parametric functions. For neutral- B background, the signal Δt resolution model is assumed.

The Dalitz plot of the continuum events is parametrized with an empirical shape, extracted from on-resonance events selected in the m_{ES} sidebands and corrected for feed-through from B decays. The continuum Δt distribution is parameterized as the sum of three Gaussian distributions with common mean and three distinct widths that scale the Δt per-event error, all determined by the fit.

IV. RESULTS

The maximum-likelihood fit results in a $B^0 \rightarrow \pi^+\pi^-\pi^0$ event yield of 1847 ± 69 , where the error is statistical only. For the U and I coefficients, the results are given together with their statistical and systematic errors in Table IV. The signal is dominated by $B^0 \rightarrow \rho^\pm\pi^\mp$ decays. We observe an excess of $\rho^0\pi^0$ events, which is in agreement with our previous upper limit [9], and the latest measurement from the Belle collaboration [10]. The result for the $\rho(1450)$ amplitude is in agreement with the findings in τ and e^+e^- decays [5]. For the relative strong phase between the $\rho(770)$ and the $\rho(1450)$ amplitudes we find $(171 \pm 23)^\circ$ (statistical error only), which is compatible with the result from τ and e^+e^- data.

A. Systematics studies

The most important contribution to the systematic uncertainty stems from the modeling of the Dalitz plot dynamics for signal. We evaluated this by observing the difference between the true values and Monte Carlo fit results, in which events are generated based on an alternative model. The alternative fit model has, in addition, a uniform Dalitz distribution for the non-resonance events and possible resonances including $f_0(980)$, $f_2(1270)$, and a low mass S -wave σ . The fit does not find significant number of any of those decays. However, the inclusion of a low mass $\pi^+\pi^-$ S -wave component significantly degrades our ability to identify $\rho^0\pi^0$ events.

We vary the mass and width of the $\rho(770)$, $\rho(1450)$, and $\rho(1700)$ within ranges that exceed twice the errors found for these parameters in the fits to τ and e^+e^- data [5], and assign the observed differences in the measured U and I coefficients as systematic uncertainties.

To validate the fitting tool, we perform fits on large MC samples with the measured proportions of signal, continuum and B -background events. No significant biases are observed in these fits, and the statistical uncertainties on the fit parameters are taken as systematic uncertainties

"Quasi twobody" $U_{\kappa}^{\pm} = A^{\kappa} ^2 \pm \bar{A}^{\kappa} ^2$	
$U_0^+ \rho^0 \pi^0$ fit fraction	$0.237 \pm 0.053 \pm 0.043$
$U_-^+ \rho^- \pi^+$ fit fraction	$1.33 \pm 0.11 \pm 0.04$
U_0^- Direct CPV ($\rho^0 \pi^0$)	$-0.055 \pm 0.098 \pm 0.13$
U_-^- Direct CPV ($\rho^- \pi^+$)	$-0.30 \pm 0.15 \pm 0.03$
U_+^- Direct CPV ($\rho^+ \pi^-$)	$0.53 \pm 0.15 \pm 0.04$
"Quasi twobody" $I_{\kappa} = \text{Im} [A^{\kappa} A^{\kappa*}]$	
I_0 Int. Mixing CPV $\rho^0 \pi^0$	$-0.028 \pm 0.058 \pm 0.02$
I_- Int. Mixing CPV $\rho^- \pi^+$	$-0.03 \pm 0.10 \pm 0.03$
I_+ Int. Mixing CPV $\rho^+ \pi^-$	$-0.039 \pm 0.097 \pm 0.02$
"Interference" $U_{\kappa\sigma}^{\pm, \text{Re(Im)}} = \text{Re(Im)} [A^{\kappa} A^{\sigma*} \pm \bar{A}^{\kappa} \bar{A}^{\sigma*}]$	
$U_{+-}^{+, \text{Im}}$	$0.62 \pm 0.54 \pm 0.72$
$U_{+-}^{-, \text{Im}}$	$0.13 \pm 0.94 \pm 0.17$
$U_{+-}^{+, \text{Re}}$	$0.38 \pm 0.55 \pm 0.28$
$U_{+-}^{-, \text{Re}}$	$2.14 \pm 0.91 \pm 0.33$
$U_{+0}^{+, \text{Im}}$	$0.03 \pm 0.42 \pm 0.12$
$U_{+0}^{+, \text{Re}}$	$-0.75 \pm 0.40 \pm 0.15$
$U_{+0}^{-, \text{Im}}$	$-0.93 \pm 0.68 \pm 0.08$
$U_{+0}^{-, \text{Re}}$	$-0.47 \pm 0.80 \pm 0.3$
$U_{-0}^{+, \text{Im}}$	$-0.03 \pm 0.40 \pm 0.23$
$U_{-0}^{+, \text{Re}}$	$-0.52 \pm 0.32 \pm 0.08$
$U_{-0}^{-, \text{Im}}$	$0.24 \pm 0.61 \pm 0.2$
$U_{-0}^{-, \text{Re}}$	$-0.42 \pm 0.73 \pm 0.28$
"Interference" $I_{\kappa\sigma}^{\text{Re}} = \text{Re} [A^{\kappa} A^{\sigma*} - \bar{A}^{\kappa} \bar{A}^{\sigma*}]$	
I_{+-}^{Re}	$-0.1 \pm 1.9 \pm 0.3$
I_{+0}^{Re}	$0.2 \pm 1.1 \pm 0.4$
I_{-0}^{Re}	$0.92 \pm 0.91 \pm 0.4$
"Interference" $I_{\kappa\sigma}^{\text{Im}} = \text{Im} [A^{\kappa} A^{\sigma*} + \bar{A}^{\kappa} \bar{A}^{\sigma*}]$	
I_{+-}^{Im}	$-1.9 \pm 1.1 \pm 0.1$
I_{+0}^{Im}	$-0.1 \pm 1.1 \pm 0.3$
I_{-0}^{Im}	$0.7 \pm 1.0 \pm 0.3$

TABLE I: Definitions and results for the 26 U and I observables extracted from the fit. We determine the relative values of U and I coefficients to U_{+}^+ .

Another major source of systematic uncertainty is the B -background model. The expected event yields from the background modes are varied according to the uncertainties in the measured or estimated branching fractions. Since B -background modes may exhibit CP violation, the corresponding parameters are varied within appropriate uncertainty ranges.

Continuum Dalitz plot PDF is extrapolated from m_{ES} sideband, and large samples of off-resonance data with loosened requirements on ΔE and the NN are used to compare the distributions of m' and θ' between the m_{ES} sideband and the signal region. No significant differences are found. We assign as systematic error the effect seen when weighting the continuum Dalitz plot PDF by the ratio of both data sets. This effect is mostly statistical in origin.

Other systematic effects due to the signal PDFs comprise uncertainties in the PDF parameterization, the treatment of misreconstructed events, the tagging per-

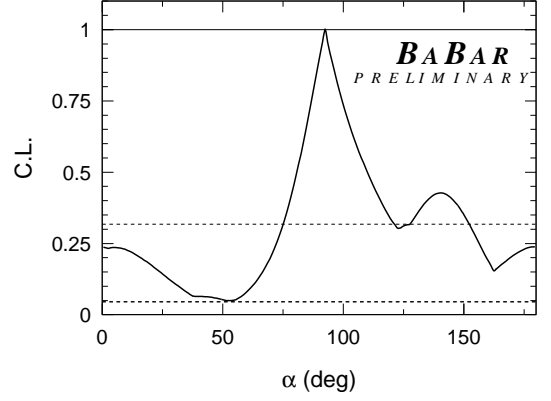


FIG. 2: Confidence level functions for α . Indicated by the dashed horizontal lines are the confidence level (C.L.) values corresponding to 1σ and 2σ , respectively.

formance, and the modeling of the signal contributions and are estimated using various data control samples.

B. Interpretation of the results

The U and I coefficients are related to the quasi-two-body parameters (Tab.IV B) defined in Ref. [4], explicitly accounting for the presence of interference effects, and are thus exact even for a ρ with finite width. The systematic errors are dominated by the uncertainty on the CP content of the B -related backgrounds. One can transform the experimentally convenient, namely uncorrelated, direct CP -violation parameters C and $\mathcal{A}_{\rho\pi}$ into the physically more intuitive quantities $\mathcal{A}_{\rho\pi}^{+-}$ and $\mathcal{A}_{\rho\pi}^{-+}$. The significance, including systematic uncertainties and calculated by using a minimum χ^2 method, for the observation of non-zero direct CP violation is at the 3.0σ level.

$C = (C^+ + C^-)/2$	$0.154 \pm 0.090 \pm 0.037$
$S = (S^+ + S^-)/2$	$0.01 \pm 0.12 \pm 0.028$
$\Delta C = (C^+ - C^-)/2$	$0.377 \pm 0.091 \pm 0.021$
$\Delta S = (S^+ - S^-)/2$	$0.06 \pm 0.13 \pm 0.029$
$\mathcal{A}_{\rho\pi} = \frac{U_{+}^+ - U_{+}^-}{U_{+}^+ + U_{+}^-}$	$-0.142 \pm 0.041 \pm 0.015$
$\mathcal{A}_{\rho\pi}^{+-} = \frac{ \kappa^{+-} ^2 - 1}{ \kappa^{+-} ^2 + 1}$	$0.03 \pm 0.07 \pm 0.03$
$\mathcal{A}_{\rho\pi}^{-+} = \frac{ \kappa^{-+} ^2 - 1}{ \kappa^{-+} ^2 + 1}$	$-0.38^{+0.15}_{-0.16} \pm 0.07$

TABLE II: Quasi twobody parameters definition and results, where $C^{\pm} = \frac{U_{\pm}^{\pm}}{U_{\pm}^{\pm}}$ and $S^{\pm} = \frac{2I_{\pm}^{\pm}}{U_{\pm}^{\pm}}$; $\kappa^{+-} = (q/p)(\bar{A}^-/A^+)$ and $\kappa^{-+} = (q/p)(\bar{A}^+/A^-)$, so that $\mathcal{A}_{\rho\pi}^{+-}$ ($\mathcal{A}_{\rho\pi}^{-+}$) involves only diagrams where the ρ (π) meson is emitted by the W boson. $\mathcal{A}_{\rho\pi}^{+-}$ and $\mathcal{A}_{\rho\pi}^{-+}$ are evaluated as $-\frac{\mathcal{A}_{\rho\pi} + C + \mathcal{A}_{\rho\pi} \Delta C}{1 + \Delta C + \mathcal{A}_{\rho\pi} C}$ and $\frac{\mathcal{A}_{\rho\pi} - C - \mathcal{A}_{\rho\pi} \Delta C}{1 - \Delta C - \mathcal{A}_{\rho\pi} C}$. Their correlation coefficient is 0.62.

The measurement of the resonance interference terms allows us to constrain the relative phase $\delta_{+-} = \arg(A^{+\ast}A^-)$ between the amplitudes of the decays $B^0 \rightarrow \rho^-\pi^+$ and $B^0 \rightarrow \rho^+\pi^-$. This constraint can be improved with the use of strong isospin symmetry. The amplitudes A^κ represent the sum of tree-level (T^κ) and penguin-type (P^κ) amplitudes, which have different CKM factors. Here we denote by $\bar{\kappa}$ the charge conjugate of κ , where $\bar{0} = 0$. We define [11] $A^\kappa = T^\kappa e^{-i\alpha} + P^\kappa$ and $\bar{A}^\kappa = T^{\bar{\kappa}} e^{+i\alpha} + P^{\bar{\kappa}}$, where the magnitudes of the CKM factors have been absorbed in the T^κ , P^κ , $T^{\bar{\kappa}}$ and $P^{\bar{\kappa}}$. Using strong isospin symmetry and neglecting isospin-breaking effects, one can identify $P^0 = -(P^+ + P^-)/2$ and 9 unknowns have to be determined by the fit.

We find for the solution that is favored by the fit $\delta_{+-} = (34 \pm 29)^\circ$, where the errors include both statistical and systematic effects, but only a marginal constraint on δ_{+-} is obtained for C.L. < 0.05 .

Finally, following the same procedure, we can also derive a constraint on α . The resulting C.L. function versus α is given in Fig. 2 and includes systematic uncertainties. Ignoring the mirror solution at $\alpha + 180^\circ$, we find $\alpha \in (75^\circ, 152^\circ)$ at 68% C.L. No constraint on α is achieved at two sigma and beyond.

V. CONCLUSIONS

We have presented the preliminary measurement of CP -violating asymmetries in $B^0 \rightarrow \pi^+\pi^-\pi^0$ decays dom-

inated by the ρ resonance. The results are obtained from a data sample of 346 million $\Upsilon(4S) \rightarrow B\bar{B}$ decays. We perform a time-dependent Dalitz plot analysis. From the measurement of the coefficients of 26 form factor bilinears we determine the three CP -violating and two CP -conserving quasi-two-body parameters, where we find a 3.0σ evidence of direct CP violation. Taking advantage of the interference between the ρ resonances in the Dalitz plot, we derive constraints on the relative strong phase between B^0 decays to $\rho^+\pi^-$ and $\rho^-\pi^+$, and on the angle α of the Unitarity Triangle. These measurements are consistent with the expectation from the CKM fit [12].

Acknowledgments

The author wishes to thank the conference organizers for an enjoyable and well-organized workshop. This work is supported by the Istituto Nazionale di Fisica Nucleare (INFN) and the United State Department of Energy (DOE) under contract DE-AC02-76SF00515.

-
- [1] H.R. Quinn and A.E. Snyder, Phys. Rev. **D48**, 2139 (1993).
- [2] H.J. Lipkin, Y. Nir, H.R. Quinn and A. Snyder, Phys. Rev. **D44**, 1454 (1991).
- [3] W. M. Yao *et al.* [Particle Data Group], J. Phys. G **33** (2006) 1.
- [4] BABAR Collaboration (B. Aubert *et al.*), Phys. Rev. Lett. **91**, 201802 (2003); updated preliminary results at BABAR-PLOT-0055 (2003).
- [5] ALEPH Collaboration, (R. Barate *et al.*), Z. Phys. **C76**, 15 (1997); we use updated lineshape fits including new data from e^+e^- annihilation [13] and τ spectral functions [14] (masses and widths in MeV/c^2): $m_{\rho^\pm(770)} = 775.5 \pm 0.6$, $m_{\rho^0(770)} = 773.1 \pm 0.5$, $\Gamma_{\rho^\pm(770)} = 148.2 \pm 0.8$, $\Gamma_{\rho^0(770)} = 148.0 \pm 0.9$, $m_{\rho(1450)} = 1409 \pm 12$, $\Gamma_{\rho(1450)} = 500 \pm 37$, $m_{\rho(1700)} = 1749 \pm 20$, and $\Gamma_{\rho(1700)} \equiv 235$.
- [6] G.J. Gounaris and J.J. Sakurai, Phys. Rev. Lett. **21**, 244 (1968).
- [7] P. Gay, B. Michel, J. Proriot, and O. Deschamps, “*Tagging Higgs Bosons in Hadronic LEP-2 Events with Neural Networks.*”, In Pisa 1995, New computing techniques in physics research, 725 (1995).
- [8] BABAR Collaboration, B. Aubert *et al.*, Phys. Rev. **D66**, 032003 (2002).
- [9] BABAR Collaboration (B. Aubert *et al.*), Phys. Rev. Lett. **93**, 051802 (2004).
- [10] Belle Collaboration (J. Dragic *et al.*), Phys. Rev. **D73**, 111105 (2006).
- [11] The BABAR Physics Book, Editors P.F. Harrison and H.R. Quinn, SLAC-R-504 (1998).
- [12] M. Bona *et al.*, JHEP, 0507 (2005) 028, J. Charles *et al.*, Eur. Phys. J. **C41**, 1 (2005).
- [13] R.R. Akhmetshin *et al.* (CMD-2 Collaboration), Phys. Lett. **B527**, 161 (2002).
- [14] ALEPH Collaboration, ALEPH 2002-030 CONF 2002-019, (July 2002).

4th International Workshop on

CKM

Unitarity Triangle

2006 Nagoya

